Kazakh Mathematical Journal ISSN 1682–0525

24:1 (2024) 14–25

The model of contact erosion at a non-stationary arc spot

Stanislav N. Kharin[1], Yuriy R. Shpadi[2]

[1,2]Institute of Mathematics and Mathematical Modeling, Almaty, Kazakhstan

[1]staskharin@yahoo.com, [2]yu-shpadi@yandex.ru

Communicated by: Altynshash Zh. Naimanova

Received: 17.12.2024 ⋆ Accepted/Published Online: 17.02.2025 ⋆ Final Version: 17.12.2024

Abstract. The model of arc evolution and instability based on the dynamics of the arc root is presented in this paper. We show that heating of a cathode material and the ejection of metallic vapors from the cathode to plasma increases arc resistivity and entails arc instability at certain critical current. As a special case, we consider phenomenon of the arc-to glow transition in low current inductive electrical circuits due to arc instability.

Keywords. Electrical contacts, arc erosion, mathematical model, Stefan problem.

1 Introduction

The problem of arc erosion in opening electrical contacts is very important for the endurance and reliability of various relays, circuit breakers, plasma generators, and many other electrical apparatuses. The dynamics of contact opening can be divided into several stages. The first one $(0 < t < t_p)$ is the pre-arcing stage, which includes the start of the contact separation and subsequent liquid metallic bridge with the length l_p rupturing at the boiling voltage U_p (Fig.1). Then the arc ignites and does not move instantly away, but remains immobile at the contacts for a certain time $t_p < t < t_i$ during which voltage rises up to the value U_i. The time $t_i - t_p$ is determined as the initial immobility time of the arc [1], or as the arc immobility period [2], or as the time of the reduced arc motion [3]. The next stage $t_i < t < t_r$ of the arc root motion from the center to the edge of the contact surface is called the edge immobility time of the arc [1] or the arc running time [2, 3]. This stage is characterized by more rapid increase of the arc voltage. It was found [4, 5, 6] that a critical contact gap l_i is required for the beginning of the arc root motion along the contact surface.

2010 Mathematics Subject Classification: 35C15, 35G30, 80A22

Funding: This research is funded by the Science Committee of the Ministry of Science and Higher Education of the Republic of Kazakhstan (Grant No. BR20281002).

DOI: https://doi.org/10.70474/kmj-2024-1-2

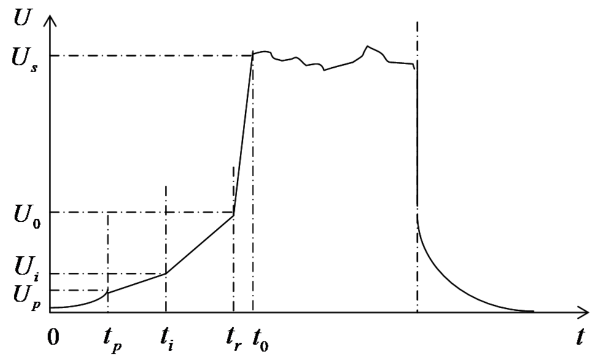

Fig.1 Stages of contact opening

Erosion of electrical contacts depends mainly on the time of the initial immobility time when the temperature on the contact spot rises rapidly up to the boiling point. The mechanism of the arc root motion is very complicated and there is no universally recognized model until now which could explain it in the general case. Arc immobility is discussed in many publications at a variety of conditions such as supplied current and voltage [3], [7], properties of a contact material [1], [3], [7], [8] circuit parameters [8], the opening velocity [1], [2], [8], the gas pressure [1] and an external magnetic field [1]. Authors tried to ascertain the outcomes of varying each parameter separately. However, the modern concept leads to the conclusion about the interdependence of all parameters; therefore, a general model describing the mechanism of arc root stagnation and further motion should take it into account.

The first part of this paper is an attempt to develop such a model in the range of low current based on the general idea that in any case the arc root leaves its spot on the contact surface and starts to move. The cause is the reduction of arc electrical conductivity due to the increase of the contact gap, the decrease of the arc temperature and evaporation rate, and insufficiency of the ionized metallic vapor to support subsequent arc burning. It is more suitable for the arc to shift to a new place (as a rule to the rim of the arc spot) where conditions for arc burning are more suitable and the power loss is minimal. Such typical arc instability can be observed in oscillograms. The result of this instability is the arc motion across the contact surface, then along runners into splitter plates with subsequent extinction. However, for some contact materials at certain circuit parameters (low current and high inductance) this instability may lead to the transformation of the arc to the glow discharge. This phenomenon is considered in the second part of this paper.

2 The model of the arc erosion

In the range of low current, the magnetic force acting on the arc root can be neglected; therefore, evaporation is the main factor responsible for arc erosion. At the initial stage of arcing, metallic vapor moves toward the arc column and, being ionized, increases the arc electrical conductivity. In spite of the fact that the distance between contacts increases at contact separation, the arc temperature rises and the rate of evaporation can sustain arc burning. E. Belbel [6] presented a model with ionized vapor jets for interpretation of arc erosion in the range of high current. It can explain qualitatively that the arc root is not able to move in a transverse magnetic field until the contact gap reaches a critical value, at which the arc voltage and resistance rise rapidly and the arc root shifts to a new location where the conditions for electrical conductivity are more convenient. Unfortunately, this model cannot be used for mathematical calculation, especially in the range of low current where vapor jets and the magnetic field should be neglected. To estimate the dynamics of the arc erosion we should develop a mathematical model describing the dynamics of the arc and contact temperatures, heat fluxes inside electrodes, evaporation and vapor density. This model is shown in Fig. 2. The arc occupying the region $D_A : 0 \le r \le r_b(t)$ interacts with the contact surface $z = 0$, and causes heating of electrodes. This interaction results in phase transformations of the contact material and formation of the three zones: the vapor zone D_0, the liquid zone D_1 and the solid zone D_2.

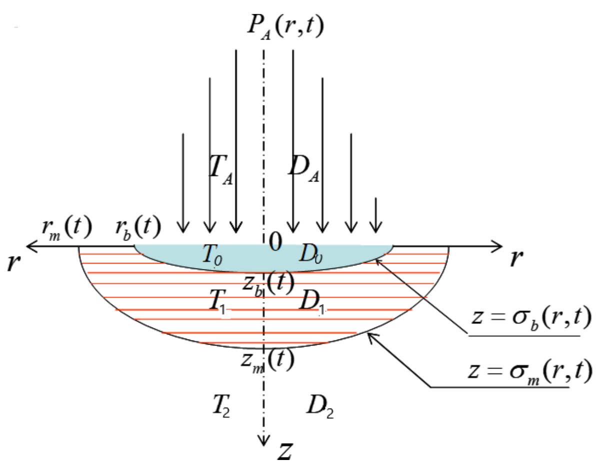

Fig.2 Interaction between arc and contact surface: arc region D_A, evaporated zone D_0, molten zone D_1 and solid zone D_2

The temperature field $T_i(r, z, t)$ inside the electrical contacts can be described in the axisymmetric model by the heat equation

$$c_i \gamma_i \frac{\partial T_i}{\partial t} = div(\lambda_i \, grad \, T_i), \quad i = 1, 2, \tag{1}$$

where c_i, γ_i, λ_i are the heat capacity, the density and heat conductivity, the index $i = 1$ corresponds to the liquid zone

$$D_1(\sigma_m(r,t) < z < \sigma_b(r,t), \quad r_m(t) < r < r_b(t))$$

and the index $i = 2$ agrees to the solid zone

$$D_2(\sigma_m(r,t)) < z < \infty, \quad r_m(t) < r < \infty$$

Here $z = \sigma_m(r,t)$ and $z = \sigma_b(r,t)$ are isothermal surfaces of melting and boiling, correspondingly, $r_m(r,t)$ and $r_b(r,t)$ are their radii on the contact surface $z = 0$.

The initial condition for the solid zone

$$T_2(r,z,0) = f(r,z), \quad 0 < r < \infty, \quad 0 < z < \infty \tag{2}$$

can be obtained by the solution of the heat equation on the stage preceding the melting at the time when the temperature at the origin $r = 0$, $z = 0$ reaches the melting value. The liquid zone at the initial time collapses into the origin where the temperature is equal to the melting value. The boundary condition on the contact plane is

$$-\lambda_1 \left.\frac{\partial T_1}{\partial z}\right|_{z=0} = \begin{cases} P(r,t), & 0 < r < r_a(t) \\ 0, & r \geq r_a(t) \end{cases} \tag{3}$$

where $P(r,t)$ is the arc heat flux and $r_a(t)$ is the arc radius. At infinity

$$T_2|_{r^2+z^2} = 0. \tag{4}$$

On the interfaces of melting and evaporation, we have

$$T_1(r,\sigma_m(r,t),t) = T_2(r,\sigma_m(r,t),t) = T_m, \tag{5}$$

$$T_1(r,\sigma_b(r,t),t) = T_b. \tag{6}$$

Finally, on these interfaces the Stefan conditions should be written

$$-\lambda_1 \left.\frac{\partial T_1}{dz}\right|_{z=\sigma_m(r,t)} = -\lambda_2 \left.\frac{\partial T_2}{dz}\right|_{z=\sigma_m(r,t)} + L_m\gamma_1\frac{\partial\sigma_m(r,t)}{\partial t}, \tag{7}$$

$$-\lambda_1 \left.\frac{\partial T_1}{dz}\right|_{z=\sigma_b(r,t)} = L_b\gamma_2\frac{\partial\sigma_b(r,t)}{\partial t}. \tag{8}$$

where L_m and L_b are latent heats for melting and for vaporization correspondingly.

We suggest that the arc heat flux $P(r,t)$ entering the electrode and the fluxes for phase transformation

$$P_m(r,t) = L_m\gamma_1\frac{\partial\sigma_m(r,t)}{\partial t} \text{ and } P_b(r,t) = L_b\gamma_1\frac{\partial\sigma_b(r,t)}{\partial t}$$

obey the normal Gauss's radial distribution

$$P(r,t) = P_A(t)\exp\left(-\frac{r^2}{r_A^2(t)}\right), \quad P_b(r,t) = P_b(t)\exp\left(-\frac{r^2}{r_A^2(t)}\right),$$

$$P_m(r,t) = P_m(t)\exp\left(-\frac{r^2}{r_A^2(t)}\right) \tag{9}$$

If $P_A(t)$ is known, then the solution of this Stefan problem with two free boundaries can be found using the method of majorant functions expounded in detail in [9], and the expression for the contact temperature can be written in the form [10]

$$T(r,z,t) = \frac{a}{\lambda\sqrt{pi}}\int_0^t \frac{[P_A(t_1) - P_b(t_1) - P_m(t_1)]r_A^2(t_1)}{[r_A^2(t_1) + 4a^2(t-t_1)]\sqrt{t-t_1}} \times$$
$$\times \exp\left[-\frac{z^2}{4a^2(t-t_1)} - \frac{r^2}{r_A^2(t_1) + 4a^2(t-t_1)}\right]dt_1 \tag{10}$$

In this expression $a = \sqrt{\lambda/C\gamma}$, $r_A(t)$ is the radius of the arc root, $P_b(t) = 0$ in the time interval $t_m < t < t_b$ and $P_m(t) = 0$ in the time interval $0 < t < t_m$, where t_m and t_b are the initial times of melting and boiling respectively. To find $P_A(t)$ we should complete the mathematical model by the equation for the arc temperature $T_A(t)$ averaged across its volume V in the following way:

$$CV\frac{dT_A}{dt} + Q(t) = Q_A(t) \tag{11}$$

where $Q(t) = \pi r_A^2(t)P(t)$ $Q(t) = \pi r_A^2(t)P_A(t)$ and also, by generalized Mayr and Cassie equations for the arc electrical conductance and power balance on the anode and cathode surfaces, which are described in the paper [11]. Then the geometry and the volume of the evaporated zone D_0 can be estimated using the values $r_b(t) = 0$ and $z_b(t) = 0$, which can be found from the equations

$$T(r_b(t), 0, t_i) = T_b, \quad T(0, z_b(t), t_i) = T_b, \tag{12}$$

where T_b is the boiling temperature. After that we can calculate dynamics of the vapor density in the arc column and electric conductivity using the method described in [12] and finally the time of arc immobility, when the arc resistance rises rapidly.

This model can be simplified if we accept two assumptions:

1) $r_A(t) = r_b(t)$, in other words, the arc root is based on the evaporating zone D_0 (this condition is used very often [12]); 2) The total power generated by arc $Q(t) = I_A(t)U_A(t)$ is distributed in equal parts to the anode and to the cathode; this assumption is correct if the arc length is not too long.

In this case, putting in the expression (10) $P_A(t) \cdot \pi r_A^2(t) = 0.5Q(t) = 0.5I_A(t)U_A(t)$, $z = 0$, $r = r_A(t)$, $T(r_A(t), 0, t) = T_b$ we obtain the integral equation for the arc radius $r_A(t)$

$$T_b = \frac{a}{2\lambda\pi^{3/2}} \int_0^t \frac{I_A(t_1)U_A(t_1)}{[r_A^2(t_1) + 4a^2(t - t_1)]} \exp\left[-\frac{r_A^2(t_1)}{[r_A^2(t_1) + 4a^2(t - t_1)]}\right] dt_1 \qquad (13)$$

3 Results of calculation

Experiments have been carried out for $AgCdO$ contacts in air at atmosphere pressure and for Ni contacts in a chamber at varied pressure. The values of measured parameters for both contact materials are given in the Tables 1 and 2.

Table 1: Ranges of measured parameters

Parameters	$AgCdO$	Ni
Supplied voltage U, V	20 – 100	48–250
Initial current I, A	0.8 – 2.0	0.5 – 3.0
Load resistance R, Ω	20–100	70–220
Load inductance L, mH	100–340	800 – 2300
Circuit capacitance C, nF	0.2 – 9.0	–
Wires resistance $R_W, m\Omega$	20–100	–
Wires inductance L_W, mH	2 – 5	–
Opening velocity $V, m/s$	0.05–0.75	0.2 – 0.3
Pressure $P, 10^5 Pa$	1.0	0.1 – 1.0

Table 2: Initial conditions for the arc

Parameters	$AgCdO$	Ni
Current I_0, A	1.6	1
Voltage U_0, V	14	15
Number density of metallic vapours $n_0, 10^{21} m^{-3}$	2.7	0.2
Contact gap, μm	8	0.03
Electric field, $10^8 V/m$	1.6	95
Arc radius, μm	45	15

Electrical circuit diagram of the test rig is presented in Fig. 3.

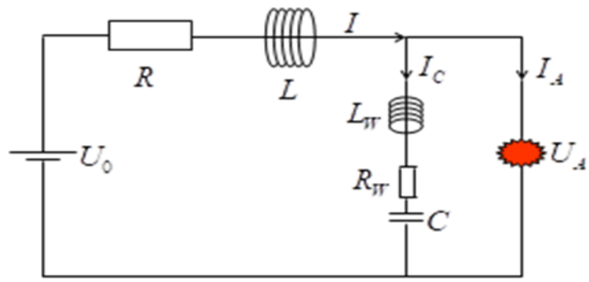

Fig.3 Electrical circuit

The special program has been elaborated to provide the computer-controlled contact separation. It enables synchronization of the motion of both contact pieces with the same acceleration at the beginning of the operation and to delay their separation up to the time required for overcoming the initial inertia and the separation with constant velocity. The results of the calculation for $AgCdO$ are presented in Fig. 4-–7.

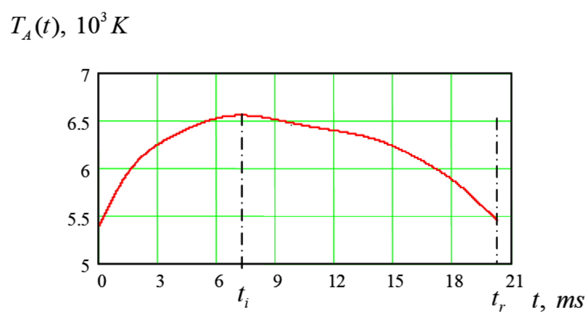

Fig.4 Dynamics of the arc temperature

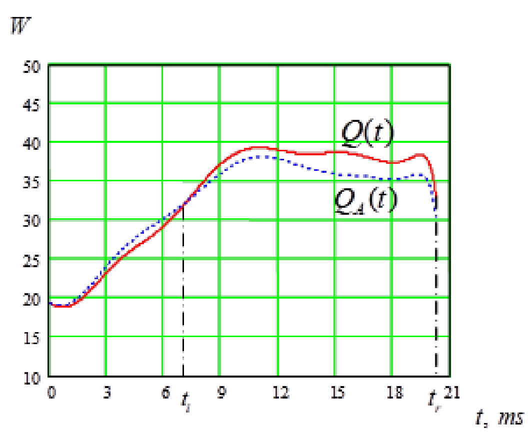

Fig.5 Arc power $Q_A(t)$ and power passing through arc root $Q(t)$

The arc temperature in Fig.4 rises up to the value $T_A = 6520K$ at $t_i = 7.2ms$, that corresponds the contact gap $l_i = 0.72mm$. Then it decreases and at the time $t_r = 20.25ms$ approaches the minimum value of gas ionization. It can be explained by the dynamics of the power components in the equation (4) which are presented in Fig. 5. If $t < t_i$, then $\frac{dT_A}{dt} > 0$ and $Q_A(t) > Q(t)$, i.e. the contact is heating. If $t > t_i$, then $\frac{dT_A}{dt} < 0$ and $Q_A(t) < Q(t)$, i.e. the contact is cooling.

The dynamics of the arc root radius calculated according to the integral equation (6) and the contact resistance are shown in Fig. 6 and in Fig. 7.

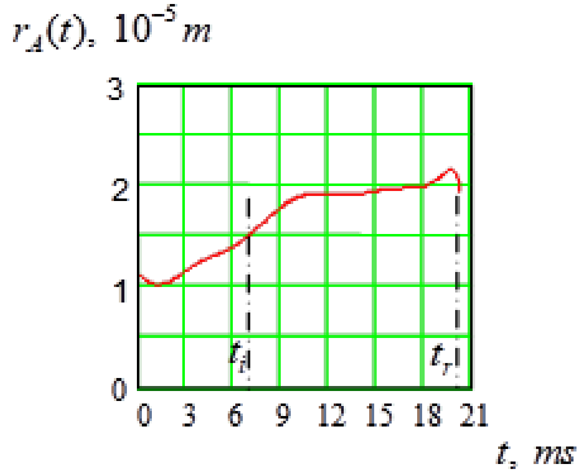

Fig.6 Dynamics of the arc root radius

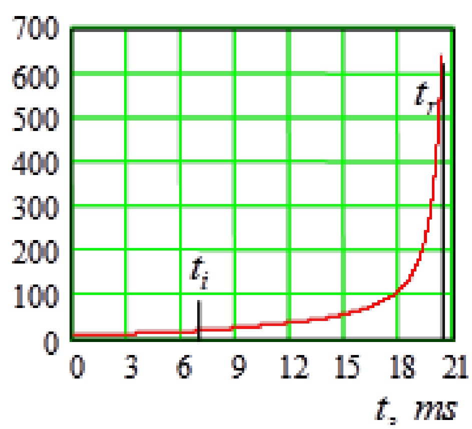

Fig.7 Dynamics of the arc resistance

One can see that just after $t = t_i$ the radius continues to rise for some time due to the thermal inertia; however, then its motion becomes slower and goes down due to the solidification of the molten pool at $t = t_r$. The arc resistance increases rapidly from the time of the arc root immobility $t = t_i$ to the arc running time $t = t_r$. The critical distance for the arc immobility is $l = 0.72mm$, this is in good agreement with other experimental data [1], [3], [7]. Similar results are obtained for Ni. However, the time of the arc immobility in this case is considerably greater.

Our analysis shows that the main role played here is the thermo-physical properties of the contact material. In particular, the pre-arcing stage and the length of the ruptured bridge are very important for the critical distance of the arc immobility l_i, which is the sum of the initial contact gap after bridging l_b and the contact path after the arc ignition $l_a : l_i = l_b + l_a$. Since l_b for Ni is less than for $AgCdO$, the value l_a should be greater to get the required critical distance l_i.

4 Arc-to-glow transition

It was mentioned above that sometimes just after the stage of the arc running, the arc-to-glow transition may occur rather than the arc extinction. This phenomenon was described in detail in [13]. It was found that such transition appears in low current inductive circuits and is accompanied by a step of spasmodic voltage increase and current decrease with duration $10^{-7} - 10^{-6}s$. (Fig. 8).

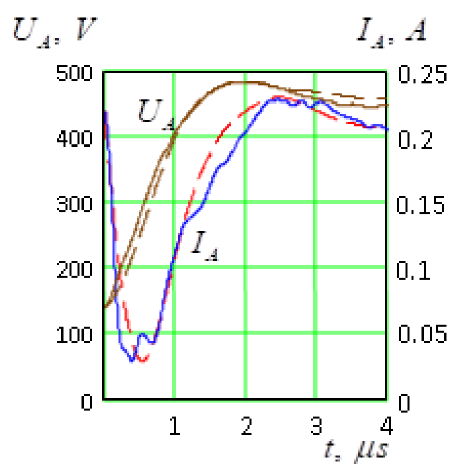

Fig.8 Transition voltage and current. $AgCdO$ contacts, $I_{cr} = 0.22A$,
dashed – calculation, solid – experiment

At certain conditions, the arc stage duration becomes much smaller than the glow stage duration. The problem is to find a criterion and an optimal choice of the interdependent parameters (material properties, current, voltage, resistance, inductance, pressure, opening velocity, etc.) providing arc instability and controlled arc-to-glow transformation. Such information is very important because new resources for the diminution of failure and for enhancement of time life and reliability of electrical contacts may be found due to the reduction of the arc duration at the expense of enlarging the glow duration, which burns practically without erosion. The conditions of the arc instability from the electrical point of view in terms of circuit parameters can be written in the form [13] (See Table 1 and Fig. 3)

$$\frac{R}{L} + \frac{1}{CR_A} - \frac{1}{\tau} < 0, \tag{14}$$

$$\frac{R}{R_A} - 1 < 0, \tag{15}$$

$$\left(\frac{R}{L} + \frac{1}{CR_A} - \frac{1}{\tau}\right)\left(\frac{1}{LC} + \frac{R}{LCR_A} + \frac{1}{\tau CR_A} - \frac{R}{LC}\right) - \frac{1}{\tau LC}\left(\frac{R}{R_A} - 1\right) < 0, \tag{16}$$

where $\tau = \frac{C_A V_A T_A}{P_A}$, V_A is arc volume, T_A is arc temperature, P_A is arc power, C_A is heat capacity of the arc, then the probability of an arc discharge transition to a glow discharge increases significantly.

The model of the arc root immobility described above enables us to interpret the phenomenon of the arc-to-glow transition from the thermophysical point of view. The decrease of the arc conductivity and increase of the arc resistance depend essentially on the properties of a metallic vapor. The time of the arc immobility and start of the running arc $t = t_i$ relates to the time of the transition from the heated arc to the cooled arc and can be found from the equations

$$\frac{dT}{dt} = 0 \quad \text{or} \quad P(t) = P_A(t). \tag{17}$$

Dynamics of the arc resistance defines an occasion of the arc-to-glow transition which occurs if the current at this time is greater than the minimal arc current. Thus, thermophysical and electrical properties of the metal vapor in the arc should be taken into account to provide the required transition with minimal time of the arc immobility.

5 Conclusion

1. The arc root immobility is conditioned by the dynamics of the contact evaporation and the arc resistivity, which depend on the vapor density in the arc.

2. The time and the critical contact distance of the arc root immobility can be found from the conditions (10) defining the change of the direction of heat fluxes into the arc for the opposite vector.

3. The axisymmetric model based on Stefan's problem with two interfaces of phase transformation enables finding the dynamics of arc power, temperature, radius, and resistance required for the calculation of parameters of arc immobility.

4. Dynamics of the arc immobility depends on the thermal and electrical properties of a contact material which should be analyzed not only at arcing but at the pre-arcing stage as well.

5. Arc-to-glow transition can be interpreted from the thermophysical point of view as the arc instability due to inefficiency of the metallic vapor in the arc column. Conditions for electric circuit parameters providing successful arc-to-glow transition should be complemented by thermophysical analysis at arcing.

References

[1] Kharin S.N., Nouri H., Miedzinski B. *Phenomena of Arc Root Immobility in Electrical Contacts*, Proceedings of the 58th IEEE Holm Conference on Electrical Contacts, Portland, OR, USA, 2012, pp. 11-15.

[2] McBride J.W., Weaver P.M., Jeffery P. *Arc Root Mobility During Contact Opening at High Current*, IEEE Transactions on CPMT, Vol 22, No 2, June 1999, pp. 344-352

[3] Manhart H., Rieder W. *Arc Mobility on New and Eroded Ag/CdO and Ag/SnO2 Contacts*, Proc. 34th IEEE Holm Conference on Electrical Contacts, 1988, pp. 47- 56.

[4] Hirose K. *Immobility Phenomena of the DC Electric Arc of Large Current Driven by a Magnetic Field*, ETJ of Japan V7(2), 1962, pp. 58-64.

[5] Belbel E.M., Lauraire M. *Behaviour of Switching Arc in Low-voltage Limiter Circuit Breakers*, IEEE Trans. CHMT. Vol. 8, No1, 1985, pp. 3-12.

[6] Belbel E., Siffroe L. *Immobility Duration of Electric Arcs Between Contactor Poles at Breaking Instant*, Proc. 30th IEEE Holm Conference on Electrical Contacts, 1982, pp. 168-170.

[7] Manhart H., Rieder W. *Erosion Behavior and Erodibility of Ag/CdO and Ag/SnO2 Contacts Under AC 3 and AC 4 Test Conditions*, Proc. 35th IEEE Holm Conference on Electrical Contacts, 1989, pp. 43-52.

[8] Chabrerie J.P., Devautour J. *Contribution to the Study of Interaction Between anAtmospheric Pressure Arc Root and Cu, Ag, or AGMO ElectrodesProc*, Proc. 36th IEEE Holm Conference on Electrical Contacts, 1990, pp. 27-34

[9] Kharin S.N. *The Method of Majorant Functions for Calculation of the Arc Erosion*, Proc. of 65th IEEE Holm Conference on Electrical Contacts, Milwaukee, 15-18 September, WI, USA, 2019 , pp.82-88.

[10] Kharin S.N. *Mathematical models of phenomena in electrical contacts*, The Russian Academy of Sciences, Siberian Branch, A.P. Ershov Institute of Informatics System, Novosibirsk, 2018, pp. 1-219.

[11] Kharin S.N. *Mathematical Model of Electrical Arc Dynamics on the Base of Cylindrical Stefan's Problem with Two Free Boundaries*, Mathematical Journal, No 1, Almaty, 2001, pp. 34-46.

[12] Zhukov M.F. *Theory of Thermo–Electrical Arc Plasma*, Edition "Nauka", Novosibirsk, 1987, pp. 285.

[13] Kharin S.N., Nouri H., Miedzinski B., Wisniewski G. *Transient Phenomena of Arc to Glow Discharge Transformation at Contact Opening*, Proc. 21st International Conference on Electrical Contacts, 2002, pp. 425-431.

Харин С.Н., Шпади Ю.Р. КОНТАКТIЛI ЭРОЗИЯ ҮЛГIСI СТАНСАЛЫҚ ЕМЕС ДОҒАЛЫ ДАҚТА

Доға түбiрiнiң динамикасына негiзделген доға эволюциясы мен тұрақсыздық моделi осы қағазда берiлген. Катодты материалды қыздыру және металл булардың катодтан плазмаға шығарылуы доғалық резистенцияны арттырады және белгiлi бiр сыни ток кезiнде доғалық тұрақсыздыққа әкеледi. Доғаның тұрақсыздығы салдарынан төмен ток индуктивтi электр тiзбектерiнде доғалы-жарқырауға ауысу құбылысы ерекше жағдай ретiнде қарастырылады.

Түйін сөздер: электр байланыстары, доға эрозиясы, математикалық модель, Стефан проблемасы.

Харин С.Н., Шпади Ю.Р. МОДЕЛЬ КОНТАКТНОЙ ЭРОЗИИ ПРИ НЕСТАЦИОНАРНОМ ДУГОВОМ ПЯТНЕ

В данной работе представлена модель эволюции и нестабильности дуги, основанная на динамике дугового канала. Показано, что нагрев материала катода и выброс паров металла с катода в плазму увеличивают удельное сопротивление дуги и приводят к нестабильности дуги при определенном критическом токе. Явление перехода дуги в тлеющее состояние в слаботочных индуктивных электрических цепях из-за нестабильности дуги рассматривается как частный случай.

Ключевые слова: электрические контакты, дуговая эрозия, математическая модель, проблема Стефана.